

Cerebral Perfusion in Acute Stroke Monitored by Time-domain Near-infrared Reflectometry

OLIVER STEINKELLNER^{1,*}, HEIDRUN WABNITZ¹,
ALEXANDER JELZOW¹, RAINER MACDONALD¹, CLEMENS GRUBER²,
JENS STEINBRINK², HELLMUTH OBRIG^{3,4}

¹ *Physikalisch-Technische Bundesanstalt, Berlin, Germany*

² *Klinik für Neurologie and Center for Stroke Research Berlin, Charité
– Universitätsmedizin Berlin, Germany*

³ *Klinik für Kognitive Neurologie, Universitätsklinik Leipzig, Germany*

⁴ *MPI für Kognitions- und Neurowissenschaften, Leipzig, Germany*

Though potentially relevant for monitoring of acute stroke, even specialized stroke units do not provide continuous methods to determine cerebral perfusion at the bedside. We present patient measurements on cerebral perfusion in ischemic stroke applying optical bolus tracking. To this end, our portable time-domain near-infrared reflectometer has been optimized and technically approved for clinical studies by a notified body. We used data analysis based on statistical moments of measured time-of-flight distributions of photons. Selective sensitivity to deep absorption changes and a suitable representation of cerebral signals is associated with the suppression of movement artifacts in severely affected patients. The proposed technique offers a unique possibility for a frequently repeatable monitoring of cerebral blood flow during acute and subacute cerebral ischemia directly at the bedside.

Key words: light propagation in tissues, time-resolved imaging, optical bolus tracking

1. Introduction

Stroke is one of the most frequent and increasingly relevant diseases in the ageing societies of developed countries. Cerebral circulatory disorders are the second most common cause of death worldwide [1]. In Europe it is the third leading cause of severe, permanent handicap and premature disability [2]. Both the personal effects as well as the economic costs are tremendous. Due to the increasing life expectancy

* Correspondence to: Oliver Steinkellner, Physikalisch-Technische Bundesanstalt, Abbestr. 2-12, 10587 Berlin, Germany, e-mail: oliver.steinkellner@ptb.de
Received 29 March 2011; accepted 13 October 2011

and the enhanced probability of suffering a stroke with age it is expected that the economic significance of the disease and its impact on life of the individual will increase further.

The faster persons affected are transferred to appropriate intensive care units, the better their prognosis. Stroke units have been shown to improve outcome in ischemic stroke, which is partly due to a much earlier diagnosis and treatment of primarily non-neurological complications. A permanent monitoring of cerebral blood flow in the first hours and days after the diagnosis is discussed as a major key to successful treatment and good rehabilitation.

Doppler sonography has been used to detect occlusion and to monitor potential success of therapy [3], but a measure of the cerebral blood flow in the infarcted area and in the surrounding penumbra is only accessible by methods that are not readily available to most stroke patients. While quantitative methods (single photon emission computed tomography, Xenon-enhanced computed tomography) [4] are not suited for repeated measurements, perfusion-weighted magnetic resonance imaging (pWMRI) based on contrast agents allows a perfusion measurement with high spatial resolution and can be repeatedly applied, in principle. However, at present and in the near future longitudinal measurement series will be restricted to few patients and to clinical research, because pWMRI necessitates to transport the patient to the magnetic resonance imager, i.e. most likely to the radiology department. It therefore interferes with continuous clinical care and is demanding with respect to costs of personnel and device. These difficulties motivate the search for alternative neuro-monitoring methods, ideally applicable continuously at the bedside, easy to use and low in cost.

Multi-channel instruments for time-domain imaging of the brain have been developed by several groups [e.g. 5–7]. They were applied in various functional stimulation experiments as well as for monitoring of cerebral perfusion by bolus tracking [8]. For the latter application, a dye bolus (indocyanine green, ICG) is intravenously administered and its passage through the sampled brain tissue is detected by an optical probe array. The suitability of optical tracking of the bolus transit by near-infrared spectroscopy (NIRS) to assess a perfusion deficit in patients with ischemic stroke has recently been demonstrated [9, 10]. The superior depth sensitivity of time-domain near-infrared spectroscopy (tdNIRS) [11] was used to monitor cerebral blood flow during acute and subacute cerebral ischemia. The procedure applied is similar to pWMRI, with the crucial advantage, that the method is portable and comparably cost-effective.

Perfusion NIRS based on ICG as a contrast agent allows a frequently repeatable measurement of the affected area. It is well suited for a longitudinal monitoring provided that an index of perfusion can be derived from a comparison of the affected with the non affected hemisphere. Such comparisons should facilitate the investigation of changes in perfusion of the infarcted area over time. It is intended to establish a quasi-continuous monitoring of cerebral perfusion for such infarcts, where the cerebral cortex is at least partially involved.

This work was carried out within the German-Polish scientific cooperation in medically oriented neuroscience, which focused on diseases of significant importance for both nations and gained considerably through the synergy of the collaborative approach to research.

2. Technical Details

Our previously developed, modularly designed tdNIRS brain imager [8] was technically modified and approved by a notified body for use in clinical trials. The instrumental arrangement, shown in Fig. 1, was configured to monitor kinetics of the ICG boluses in stroke patients by recording time-resolved diffuse reflectance. Picosecond pulses at a wavelength of 785 nm were generated by diode laser modules (BHLP-700, Becker&Hickl GmbH, Germany) with an output power of 10 mW and a repetition rate of 50 MHz. The wavelength of the laser radiation allows an efficient excitation of the contrast agent, as it is close to the absorption maximum of ICG dissolved in human blood at about 800 nm. The laser diode modules are of monolithic design and temperature stabilized. They have a fast warm-up time of about 10 minutes and a stable operating behavior that is essential in clinical trials. Two modules, one for either hemisphere, were operated simultaneously. The output of each laser module was equally split into two parts, which were coupled into multimode glass fibers of 600 μm diameter each. We used different fiber lengths, 2 m and 4 m, so that pulses from one source were delayed with respect to each other by 10 ns.

Due to the source splitting, two detection modules were sufficient to record the signals from four source-detector pairs per hemisphere simultaneously. Each detection module contained a photomultiplier tube (R7400U-02, Hamamatsu Photonics, Japan), a high voltage power supply, a preamplifier as well as relay optics.

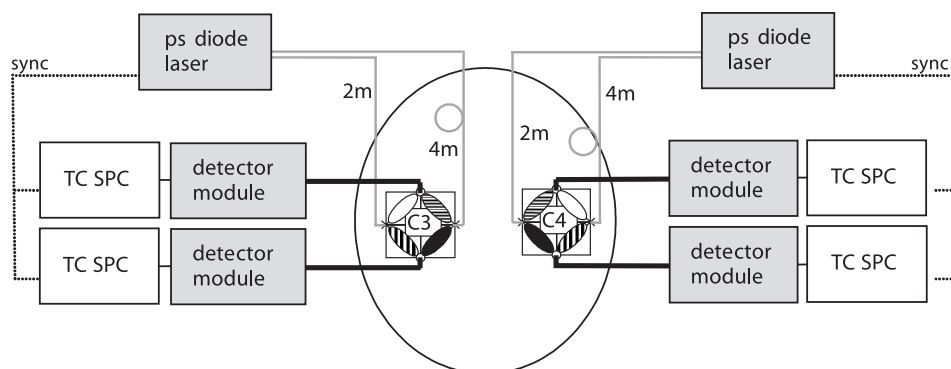


Fig. 1. The optode setup in the measurements allows direct comparison of affected and non-affected hemisphere; voxels to be compared are marked with the same fill patterns

The four detector units were connected to a multi-board time-correlated single photon counting (TCSPC) system (SPC-134, Becker&Hickl GmbH, Germany). Histograms of the detected single-photon events are accumulated in 1024 time channels of 24.4 ps width and stored every 50 ms. The count rates were adjusted between 2 MHz and 3 MHz. The instrument response function (IRF) was typically around 700 ps (FWHM) wide.

For each hemisphere two source fibers were mounted on an optode holder pad together with two detection fiber bundles (diameter 4 mm, NA 0.54, length 2 m; Loptek Glasfasertechnik, Germany). The fibers and the fiber bundles were arranged alternating on the vertices of a square with an edge length of 3 cm. Two pads, identical in construction, were placed on the head, one on each hemisphere, and securely fixed above the motor cortex regions (C3 and C4 according to the 10–20 system). Thus four voxels per hemisphere could be monitored using only two detection modules. The detection units associated to each hemisphere were triggered by the corresponding laser module. The pads and the headband were manufactured from a biocompatible neoprene material. Medical grade elastic Velcro straps ensured a secure fixation on the patient's head. The arrangement and the tightening procedure, optimized for quick and secure mounting as well as patient comfort, are sketched in Fig. 2.

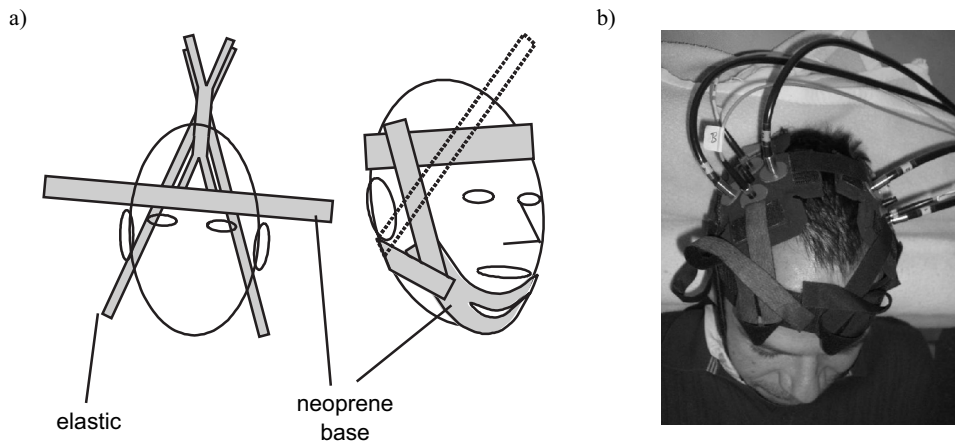


Fig. 2. (a) optode holder mounting procedure; (b) volunteer with optode pad and connected optical fibers

The fluorescence of the contrast agent ICG (peak at about 830 nm in human blood), which must be considered as a signal contamination in an absorption-based measurement, has to be suppressed efficiently. Therefore the detection modules had to be equipped with additional band pass filters (L780-10, TFI Technologies, Inc., USA). As fluorescence suppression is essential in data analysis based on moments of distributions of times of flight (DTOF, see section on ‘Data analysis’), we will

describe this issue in more details. Figure 3a and 3b display histograms recorded on a volunteer measurement. 100 histograms have been binned, therefore an average over a period of 5 s is shown. The signal at the peak of the bolus passage (solid line) is compared to a reference signal, which was recorded 2 min after the bolus passage (dashed line). As expected, the additional absorption generated by the contrast agent leads to a noticeable signal decrease. One may also expect, that due to the difference in the path length, photons with long times of flight are more suppressed than those with short ones. This has been proved, indeed, but effects on the curve shape were rather small. Moreover, a distinct signal increase was found on the trailing edge of the signal, which must be attributed to fluorescence photons emitted from the contrast agent (Fig. 3a). Due to the low fluorescence quantum yield of ICG the effect on the integrated signal can be neglected, however, it is devastating on the analysis of the waveform. Figure 3b displays a measurement on the same position with a fluorescence suppression filter inserted. The fluorescence hump was reduced successfully. To check the filtering effect, the curves from Fig. 3a have been divided by the signals from Fig. 3b. As can be seen in Fig. 3c, the filter only caused a time-independent reduction in the count rate at the reference signal (dashed line, $N_a(t)/N_b(t) \approx 1.4$), whereas the parasitic fluorescence, visible during the passage of the contrast agent, was suppressed efficiently (solid line).

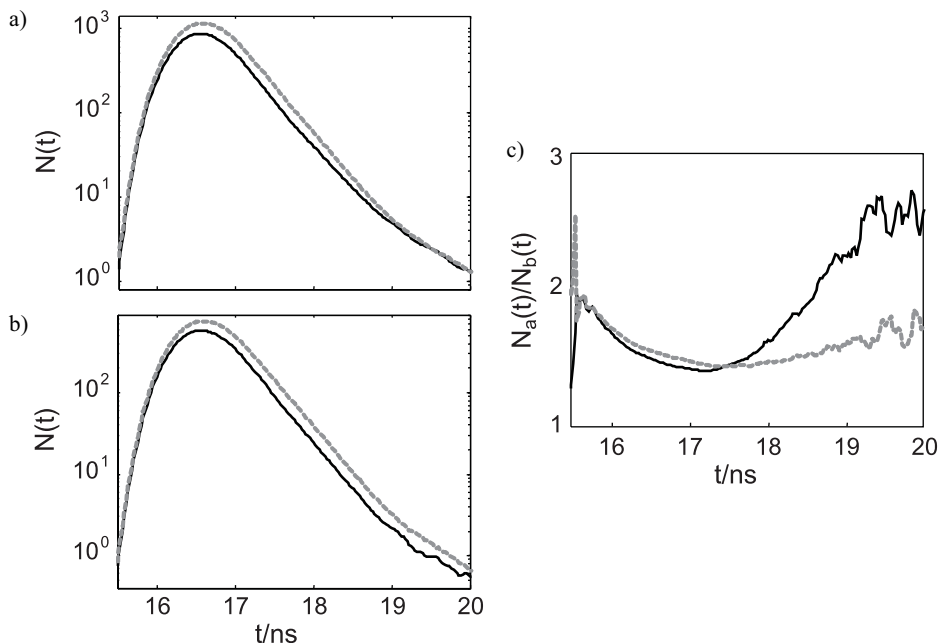


Fig. 3. DTOF from a volunteer measurement. Signal at bolus passage (solid line) was compared to a reference 2 min after the bolus (dashed line): (a) no fluorescence suppression; (b) fluorescence suppressed by filter; (c) ratio of corresponding signals from (a) to (b)

3. Clinical Details

Ten patients were recruited at two Stroke Units of the Department of Neurology of the Charité, (Berlin, Germany) from 08/2008 to 03/2009. The patients presented due to an acute hemiparesis and/or mild to moderate aphasia, compatible with a stroke in the territory of the middle cerebral artery. The mean age was 67 ± 14 ranging from 31 to 81 and both genders were equally represented. The National Institute of Health Stroke Scale (NIHSS) was between 0 and 16, with an average of 4.7. Severe aphasias and other deficits interfering with the mandatory consent procedure were excluded. Therefore the remaining NIHSS at the time of the measurement was not exceeding 5 at most patients. Exceptions were patient 4 (NIHSS 16) and patient 7 (NIHSS 10). The patients gave informed consent to the study prior to inclusion and the protocol and the procedures were approved by the local Ethical Committee. Further clinical and epidemiological details can be found in ref. [17].

The contrast agent used was ICG Pulsion® from Pulsion Medical Systems AG, Germany. In the present study we applied several boluses of 6 mg ICG diluted in 6 ml of aqua injected manually into the cubital vein. After the bolus the line was flushed with 20 ml saline. Up to four dye injections at a repetition time of about 5 minutes were performed in each patient. The doses were chosen so low, that even half hourly application for pseudo-continuous stroke monitoring would not reach the maximal daily dose of 5 mg/kg body weight recommended by the safety guidelines [12].

The measurement on a patient can be divided into two parts, the preparation and the actual perfusion measurement. In the preparatory phase the device was moved to the patient's bed at the stroke unit and switched on. During temperature stabilization of the electronics the optode pad was attached to the patient's head and readjusted if necessary. In parallel, the contrast agent was prepared. At the beginning of the perfusion measurement the transparency of each patient was determined in a recording without contrast agent. Then the main perfusion measurement was carried out as described above. Duration of the whole procedure did not exceed a half an hour.

4. Data Analysis

The analysis is related to the two different time scales of the measurement, (i) the nanosecond time scale of the DTOF, which we designate by the lowercase 't' and (ii) the time scale concerning the passage of the contrast agent bolus in the range of seconds, designated by an uppercase 'T'.

Practically, the analysis started with the processing of the DTOF. After background subtraction, we calculate statistical moments m_k of the histogram $N(t)$ of diffusely reflected photons [13], $m_k = \int_{t_1}^{t_2} t^k N(t) dt$, where k is the order of the moment. The integral of the histogram, mean time of flight, i.e. the first nor-

malized moment $\langle t \rangle = m_1/m_0$, and variance, i.e. the second centralized moment $V = m_2/m_0 - (m_1/m_0)^2$ are derived. The integration limits t_1, t_2 were fixed corresponding to fractions (0.01 for t_1 and 0.03 for t_2) of the maximum photon count for the global DTOF averaged over the whole time series. A proper choice of the upper integration limit is essential, in particular for the variance. As late photons with a large time of flight correspond to long pathways through the tissue, they are most important for the sensitivity towards cortical signals. Reducing the integration range much below the value used here would lead to considerable errors in the estimation of the cortical contribution. Extending the integration range too far, however, would lead to larger uncertainties due to the background noise.

The integral number of the detected photons is strongly influenced by the optical properties in the skin. In calculating of the higher moments m_k , the histogram values are increasingly weighted by the time of the detection t^k and therefore they feature an enhanced sensitivity to the deep layers, i.e. the cortex. In addition, for the calculation of $\langle t \rangle$ and V deconvolution of the signal with the IRF can be taken into account simply by subtraction, so that changes in the moments $\Delta\langle t \rangle, \Delta V$ do not depend on the IRF. The normalized moments are independent of intensity and thus are not affected by amplitude fluctuations. Moreover, the variance does not even depend on the origin of the time axis. Drifts of the temporal position of the DTOF, which are slow compared to the collection time applied, will not influence the signal.

These features of moments are relevant for the sensitivity to instrumental fluctuations as well as for the sensitivity to motion artifacts. Figure 4 displays a 10-minute-sequence from a measurement on a patient suffering from an acute ischemic stroke.

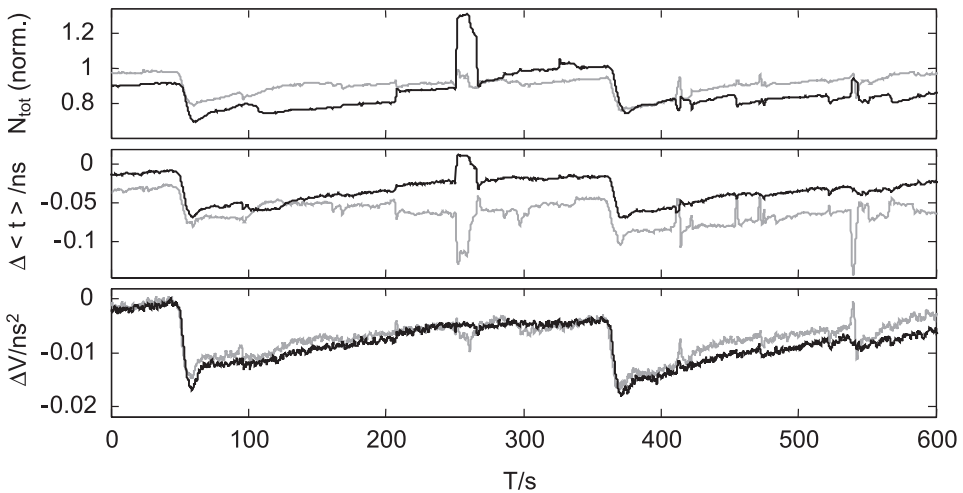


Fig. 4. Normalized moments of two selected channels from a patients measurement. Time course T contains two ICG bolus passages. The variance V suffers considerably less from motion artifacts than integral N_{tot} and mean time of flight $\langle t \rangle$

Due to the severity of the infarction, persistent unregulated motions are present. We have selected two of eight channels recorded at the same time. The time course T contains two ICG bolus injections. The channel represented by the black curve shows strong motion artifacts on the same scale as the signal intensity changes induced by the ICG bolus. Normalized moments, which do not depend on intensities are not influenced neither by instabilities in the input power nor by changes in the detection efficiency, e.g. due to changes in the coupling of the fibers to patient's skin. This effect can be seen looking at the changes in the moments $\Delta\langle t \rangle, \Delta V$ in Fig. 4: Motion artifacts are dramatically reduced in displaying of mean time of flight and even further if the variance is plotted. It has been shown, on the one hand, that the sensitivity to deeper layers is not much enhanced by the use of the variance instead of the mean time of flight [13]. As on the other hand the signal to noise ratio falls off in quality the higher the order of the moment is, it could be concluded that use of $\langle t \rangle$ would be a sufficient compromise. A different conclusion must be drawn, however, by looking at the grey curves of Fig. 4. While the signal changes assigned to motions of the patient show a minor influence on the changes in the time integrated signal ΔN_{tot} , it gains importance on the first moment $\Delta\langle t \rangle$, whereas in the variance representation these signal contributions almost vanish. From these findings it must be concluded that the analysis of the variance is the best choice.

It has to be noted that the variance is very sensitive to the slightest disturbance in the waveform. A transient fluorescence hump, delayed by some nanoseconds on the time scale 't', as presented in Fig. 3, may result in a shift of the variance signal on the time course 'T' even by seconds. Figure 5 compares bolus shapes obtained from the DTOF shown in Fig. 3 with (black line) and without (grey line) fluorescence blocking filter. While the time course T of the integral (Fig. 5a) does not show any significant influence of the filter, the variance signal (Fig. 5b) is substantially distorted. The variance is rather susceptible to the signal contaminations at late times t because they enter with larger weight. Use of a fluorescence blocking filter is therefore mandatory for a variance-based signal analysis. The integral signal is only marginally affected due to the low fluorescence quantum yield of ICG (3% in physiological environment [14]), and the low ICG concentration. In particular, the position of absorption maximum is not altered.

The macroscopic time course T is relevant for the extraction of bolus kinetics from the time series of the recorded signals. A fit of the gamma-variate function [15] was used to analyze signal changes induced by the contrast agent. The gamma-variate function with a delay serves as a model function,

$$C_0(T) = C_p \cdot \left(\frac{T - T_0}{T_p} \right)^a \cdot \exp\left(-a \cdot \frac{T - T_0}{T_p} \right), \quad \text{for } T \geq T_0, \quad (1)$$

$$= 0, \quad \text{for } T < T_0,$$

where T_p is the time to the bolus maximum and T_0 the delay from the bolus injection. Since the function $C_0(T)$ approaches zero for the short and long times T , a baseline has to be subtracted prior to fitting of Eq. 1 to the experimental data. The peak value is $C_0(TTP) = C_p \cdot \exp(-a)$ and a indicates the asymmetry of the curve. As the time courses showed a long-lived component on the trailing edge of the bolus signal, which does not correspond to the cortical bolus passage, the fit was truncated 5 s after the signal minimum. Time-to-peak, $TTP = T_p + T_0$, has proven to be a valid parameter to assess the perfusion also in case of an acute cerebral infarction [16]. The onset-time of the signal, OT, which is a measure for the delay experienced by the dye bolus, was calculated at a fraction of 0.05 of the maximum signal swing. Figure 6 illustrates the collected parameters.

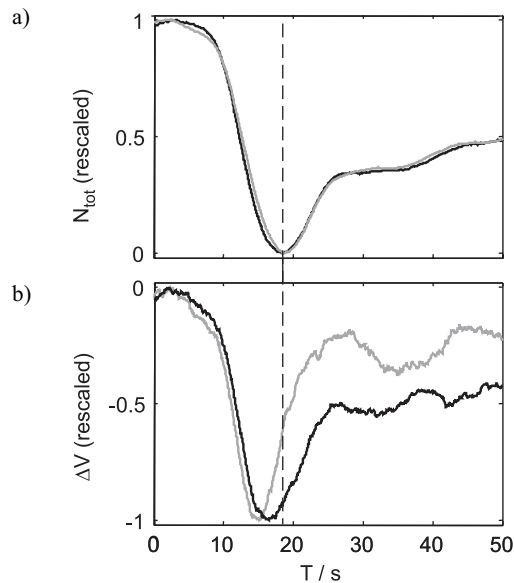


Fig. 5. Influence of fluorescence on the diffuse reflectance signals. Data from a healthy volunteer, without (grey lines) and with (black lines) the fluorescence blocking filter. (a) normalized integral N_{tot} , (b) change in the variance, ΔV

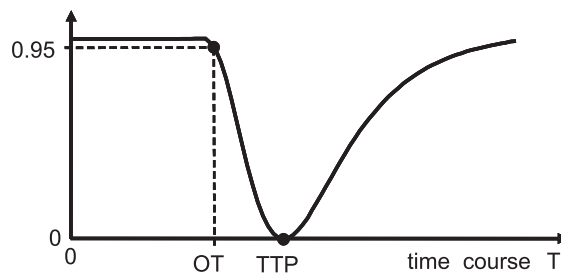


Fig. 6. Parameters collected on the macroscopic time scale T

It should be noted that in contrast to the pwMRI measurements, the arterial input function, i.e. the time course of the bolus in the artery supplying the tissue under consideration, is currently not directly accessible by our method. Therefore we focus on the analysis of differences between the affected and the unaffected hemispheres.

5. Results

In this section we first explain the advantage of our time-resolved method based on an admittedly extreme case. Then we discuss the results of ten measurements on patients, which were made during the period mentioned above. Parts of the results of this study have been recently published [17].

Figure 7 illustrates a measurement on a patient (patient 1) suspected of a hemodynamic cause of the ischemia. This patient had previously undergone a desobliteration of the internal carotid artery (ICA) on the opposite side. The vascular diagnostics revealed an ICA occlusion on the affected side and a crossflow over the anterior communicating artery (ACoA). The anatomical situation and the influence on the bolus passage are shown schematically in the illustration Fig. 7c. On the cortex the contrast agent reached the affected hemisphere (shown in black color) with a distinct delay in respect to the unaffected one (shown in light grey). The overlying skin, however,

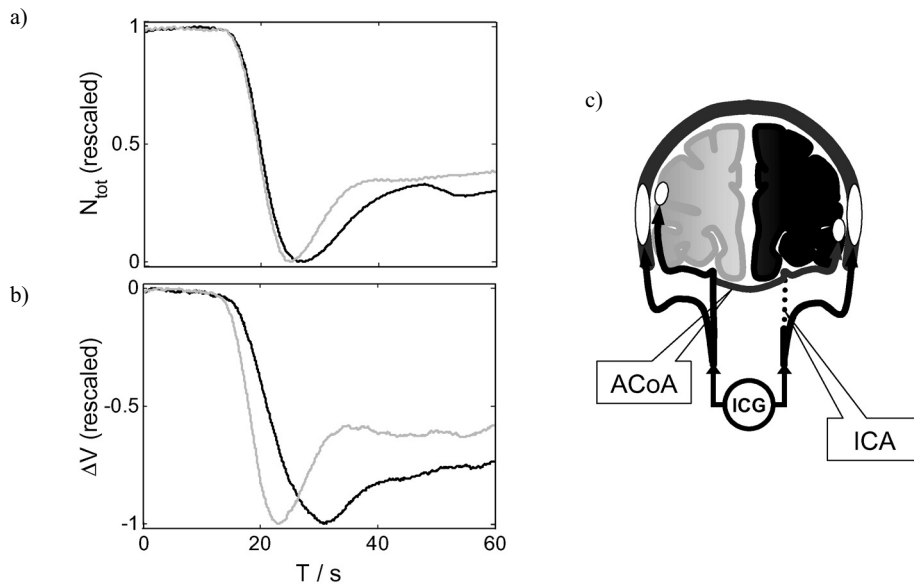


Fig. 7. Subject suffering from occlusion of the internal carotid artery (ICA) and crossflow over the anterior communicating artery (ACoA). (a) time-integrated bolus signal N_{tot} , (b) variance signal ΔV , (c) illustration of anatomy and influence on bolus passage

was supplied on both hemispheres without any significant delay. It must be assumed further, that a dye bolus moving through the skin tissue is broadened and delayed with respect to the unaffected cortex. We illustrate this by the white spots on the depiction. The left side of the figure compares the conventional cw-based approach, which is represented by the time-integrated signal N_{tot} (Fig. 7a) to our tdNIRS approach relying on variance (Fig. 7b). The colors of the bolus curves correspond to Fig 7c. At the time-integrated signal the bolus curves differed only slightly indicating that the time course seen was mostly caused by the skin. In contrast, the variance signals ΔV showed a significant difference between the hemispheres, as depicted in Fig. 7b. Comparing the Figures 7a and b with each other on basis of the time curves of the healthy hemispheres (light grey), in the variance signal the bolus appeared earlier. This is another clear sign that the time-integrated signal mainly reflected the blood flow in the skin, while this component was suppressed in the time-resolved method.

Figure 8 shows the results obtained in 10 patients measured during the acute stage of an ischemic stroke. We calculated the inter-hemispheric differences of TTP , which were derived from the ΔV time courses with the procedure described in the section ‘Data analysis’. The ΔTTP was calculated for each corresponding optode pair and each of the bolus administrations. In patients 1, 2, 3, 6 and 7 the left hemisphere was affected, in the other patients the right hemisphere. Patient 1 was the subject described in Fig. 7, the prominence of this case was demonstrated by the large delay. The TTP -difference affected-unaffected hemisphere in all but one cases revealed a delay in the bolus passage, which is in line with the assumption of an acute hypoperfusion of the affected hemisphere. In patient 6, ΔTTP had a negative sign, but the particular value was of low magnitude (-0.2 s). This deviation may be caused by the simple fitting procedure using truncated data.

In Figure 9 the measurements are presented again, however, we distinguish between the inter-hemispheric differences in onset-time (ΔOT , Fig. 9a), as a rep-

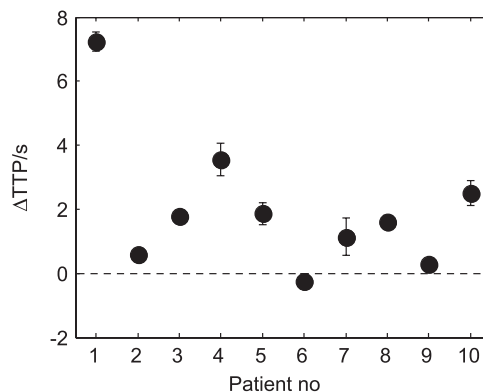


Fig. 8. Differences in times-to-peak (ΔTTP) in patients suffering from acute stroke

resentation of the delay the boluses have experienced, and the differences in the leading edges ($\Delta(\text{TTP-OT})$, Fig. 9b), calculated as the differences between time-to-peak and onset-time for each optode pair and bolus administration. The latter value mainly reflects the influence of the differences in dispersion. It becomes clear that both effects are important in assessment of a perfusion deficit, albeit in varying degrees. Here we do not focus on the clinical reasons for this variability. In view to our methodological focus it should be noticed, that the isolated value determined at patient 6 was mainly based on differences in the shape of the measured bolus, and not in the passage of the contrast agent.

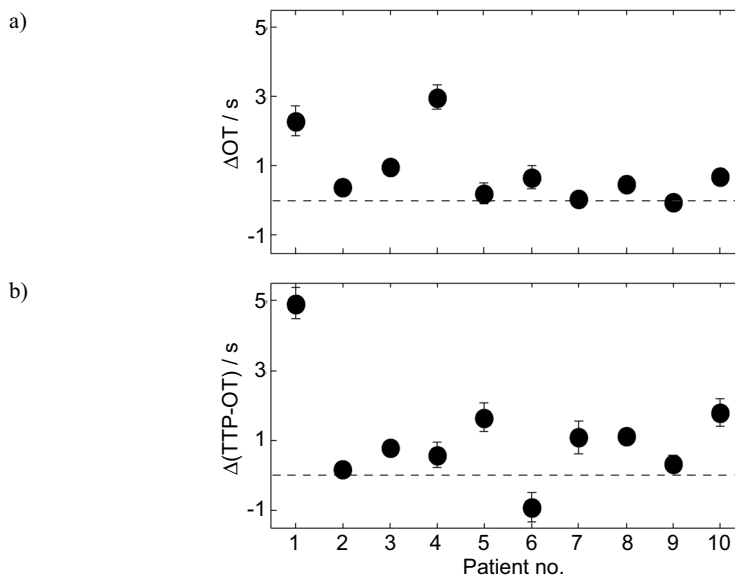


Fig. 9. Patients suffering from acute stroke. (a) differences based on delay. (b) differences based on dispersive effects

6. Conclusion

A tdNIRS approach was used to assess perfusion in the acute stroke patients directly on an intensive care unit. Analyzing changes in the optical signals caused by the intravenously administered ICG boluses, a clear difference in perfusion of the diseased hemisphere compared to the unaffected one could be observed as a relative delay. The measurement configuration consisting of four channels on either hemisphere was a reasonable trade-off between technical and clinical demands.

One more time it turned out from this clinically relevant study that the time-domain approach is more suitable to record the truly intracerebral signals when compared to already available monitors based on the cw-approach.

In the present work we have additionally shown that the time-domain approach also allows a substantial reduction of motion artifacts in the optical signals, when analyzing variance of the DTOF. However, as these signals are more susceptible to contamination by the ICG fluorescence, suppression of the residual fluorescence photons emitted from the contrast agent is necessary

Acknowledgments

The research leading to these results has received funding from the German Federal Ministry of Education and Research via the grants “Hypo- and Hyperfusion during subacute Stroke. Tracking Perfusion Dynamics in stroke Patients with Optical Imaging” (01GZ0710/01GZ0711) and “Center for Stroke Research Berlin” (01EO0801) as well as from the European Community’s Seventh Framework Programme [FP7/2007-2013] under grant agreement no. FP7-HEALTH-2008-201076.

References

1. Murray C.J.L., Lopez A.D.: Mortality by cause for eight regions of the world: Global Burden of Disease Study. *Lancet* 1997, 349, 1269–1276.
2. Murray C.J.L., Lopez A.D.: Alternative projections of mortality and disability by cause 1990-2020: Global Burden of Disease Study. *Lancet* 1997, 349, 1498–1504.
3. Molina C.A., Alexandrov A.V.: Transcranial ultrasound in acute stroke: from diagnosis to therapy. *Cerebrovasc. Dis.* 2007, 24 Suppl 1, 1–6.
4. Latchaw R.E.: Cerebral perfusion imaging in acute stroke. *J. Vasc. Interv. Radiol.* 2004, 15, S29–S46.
5. Selb J., Stott J.J., Franceschini M.A., Sorenson A.G., Boas D.A.: Improved sensitivity to cerebral hemodynamics during brain activation with a time-gated optical system: analytical model and experimental validation. *J. Biomed. Opt.* 2005, 10, 11013.
6. Contini D., Torricelli A., Pifferi A., Spinelli L., Paglia F., Cubeddu R.: Multi-channel time-resolved system for functional near infrared spectroscopy. *Opt. Express* 2006, 14, 5418–5432.
7. Kacprzak M., Liebert A., Sawosz P., Zolek N., Maniewski R.: Time-resolved optical imager for assessment of cerebral oxygenation. *J. Biomed. Opt.* 2007, 12, 034019.
8. Wabnitz H., Moeller M., Liebert A., Walter A., Erdmann R., Raitza O., Drenckhahn C., Dreier J.P., Obrig H., Steinbrink J., Macdonald R.: A time-domain NIR brain imager applied in functional stimulation experiments, in: *Photon Migration and Diffuse-Light Imaging II*, Proc. OSA-SPIE Biomed. Opt. 2005, 5859, 70–78.
9. Terborg C., Gröschel K., Petrovitch A., Ringer T., Schnaudigel S., Witte O.W., Kastrup A.: Noninvasive assessment of cerebral perfusion and oxygenation in acute ischemic stroke by near-infrared spectroscopy. *Eur. Neurol.* 2009, 62, 338–343.
10. Terborg C., Bramer S., Harscher S., Simon M., Witte O.W.: Bedside assessment of cerebral perfusion reductions in patients with acute ischaemic stroke by near-infrared spectroscopy and indocyanine green. *J. Neurol. Neurosurg. Psychiatry* 2004, 75, 38–42.
11. Liebert A., Wabnitz H., Moeller M., Macdonald R., Rinneberg H., Steinbrink J., Villringer A., Obrig H.: Bed-side assessment of cerebral perfusion in stroke patients based on optical monitoring of a dye bolus by time-resolved diffuse reflectance. *Neuroimage* 2005, 24, 425–435.
12. Raabe A., Beck J., Gerlach R., Zimmermann M., Seifert V.: Near-infrared indocyanine green video angiography: a new method for intraoperative assessment of vascular flow. *Neurosurgery* 2003, 52, 132–139, discussion 139.

13. Liebert A., Wabnitz H., Steinbrink J., Obrig H., Moller M., Macdonald R., Villringer A., Rinneberg H.: Time-resolved multidistance near-infrared spectroscopy of the adult head: intracerebral and extracerebral absorption changes from moments of distribution of times of flight of photons. *Appl. Opt.* 2004, 43, 3037–3047.
14. Licha K., Riefke B., Ntziachristos V., Becker A., Chance B., Semmler W.: Hydrophilic cyanine dyes as contrast agents for near-infrared tumor imaging: synthesis, photophysical properties and spectroscopic in vivo characterization. *Photochem. Photobiol.* 2000, 72, 392–398.
15. Madsen M.T.: A simplified formulation of the gamma variate function. *Physics in Medicine and Biology* 1992, 31, 1597–1600.
16. Yamada K., Wu O., Gonzalez R.G., Bakker D., Østergaard L., Copen W.A., Weisskoff R.M., Rosen B.R., Yagi K., Nishimura T., Sorensen A.G.: Magnetic resonance perfusion-weighted imaging of acute cerebral infarction: effect of the calculation methods and underlying vasculopathy. *Stroke* 2002, 33, 87–94.
17. Steinkellner O., Gruber C., Wabnitz H., Jelzow A., Steinbrink J., Fiebach J.B., Macdonald R., Obrig H.: Optical Bedside Monitoring of Cerebral Perfusion: Technological and Methodological Advances Applied in a Study on Acute Ischemic Stroke. *J. Biomed. Opt.* 2010, 15(6), 061708.